Runge-Kutta Time Integration and High-Order Spatial Discretization of Advection – A New Dynamical Core for the LMK

Jochen Förstner and Günther Doms

Deutscher Wetterdienst, P.O.Box 100465, 63004 Offenbach a.M., Germany

1 New Dynamical Core

LMK is the name for a new development branch of the *LM* aiming at the meso-gamma scale (horizontal resolution of 2-3 km) and shortest range ("*K*ürzestfrist") forecasts periods (3-18 h). The new dynamical core for the LMK is based on different variants of 2-timelevel Runge-Kutta schemes, which are combined with a forward-backward scheme for integrating the high-frequency modes of the elastic equations. The first one is the normal 3rd-order Runge-Kutta scheme used by Wicker and Skamarock (2002) whereas the second one is a total variation diminishing (TVD) variant of 3rd-order (Liu, Osher and Chan 1994).
For horizontal advection upwind or centered-differences schemes of 3rd- to 6th-order can be used – the operators are formulated in advection form. The vertical advection is normally treated in an implicit way using a Crank-Nicolson scheme and centered-differences in space. Most slow tendencies such as vertical diffusion, thermal/solar heating, parameterized convection and coriolis force are computed only once using values of the prognostic variables at time step n. These tendencies are fixed during the individual Runge-Kutta steps and contribute to the total slow-mode tendencies which are integrated in several small time steps together with the fast-mode tendencies in a time-splitting sense. In contradiction to this, the whole 3D-advection is computed in each Runge-Kutta step.
In the following the procedures for the two Runge-Kutta schemes are described mathematically in a simplified form – the treatment of the physical forcing terms is omitted and the only operators listed are the ones for advection.

Problem to Solve:

$$\frac{\partial \phi}{\partial t} = L^{slow}(\phi) + L^{fast}(\phi)$$

Computation of the Slow Tendency:

***Normal* 3rd-order Runge-Kutta:**

$$\begin{aligned}\phi^{*}_{i,k} &= \phi^{n}_{i,k} - \frac{1}{3}\Delta t\; L^{h}_{i}(\phi^{n}) - \frac{1}{3}\Delta t\Big(\beta^{+} L^{v}_{k}(\phi^{*}) + \beta^{-} L^{v}_{k}(\phi^{n})\Big)\\ &= \phi^{0}_{i,k} + \frac{1}{3}\Delta t\; L^{slow}_{i,k}\Big|^{*}_{0}\end{aligned}$$

$$\begin{aligned}\phi^{**}_{i,k} &= \phi^{n}_{i,k} - \frac{1}{2}\Delta t\; L^{h}_{i}(\phi^{*}) - \frac{1}{2}\Delta t\Big(\beta^{+} L^{v}_{k}(\phi^{**}) + \beta^{-} L^{v}_{k}(\phi^{*})\Big)\\ &= \phi^{0}_{i,k} + \frac{1}{2}\Delta t\; L^{slow}_{i,k}\Big|^{**}_{0}\end{aligned}$$

$$\begin{aligned}\phi^{n+1}_{i,k} &= \phi^{n}_{i,k} - \Delta t\; L^{h}_{i}(\phi^{**}) - \Delta t\Big(\beta^{+} L^{v}_{k}(\phi^{n+1}) + \beta^{-} L^{v}_{k}(\phi^{**})\Big)\\ &= \phi^{0}_{i,k} + \Delta t\; L^{slow}_{i,k}\Big|^{n+1}_{0}\end{aligned}$$

***TVD-variant* of 3rd-order Runge-Kutta:**

$$\begin{aligned}
\phi^*_{i,k} &= \phi^n_{i,k} - \Delta t\, L^h_i(\phi^n) - \Delta t\Big(\beta^+ L^v_k(\phi^*) + \beta^- L^v_k(\phi^n)\Big)\\
&= \phi^0_{i,k} + \Delta t\, L^{slow}_{i,k}\Big|^*_0
\end{aligned}$$

$$\begin{aligned}
\phi^{**}_{i,k} &= \frac{3}{4}\phi^n_{i,k} + \frac{1}{4}\phi^*_{i,k} - \frac{1}{4}\Delta t\, L^h_i(\phi^*) - \frac{1}{4}\Delta t\Big(\beta^+ L^v_k(\phi^{**}) + \beta^- L^v_k(\phi^*)\Big)\\
&= \phi^0_{i,k} + \frac{1}{4}\Delta t\, L^{slow}_{i,k}\Big|^{**}_0
\end{aligned}$$

$$\begin{aligned}
\phi^{n+1}_{i,k} &= \frac{1}{3}\phi^n_{i,k} + \frac{2}{3}\phi^{**}_{i,k} - \frac{2}{3}\Delta t\, L^h_i(\phi^{**}) - \frac{2}{3}\Delta t\Big(\beta^+ L^v_k(\phi^{n+1}) + \beta^- L^v_k(\phi^{**})\Big)\\
&= \phi^0_{i,k} + \frac{2}{3}\Delta t\, L^{slow}_{i,k}\Big|^{n+1}_0
\end{aligned}$$

Time-Splitting Method:

After each Runge-Kutta step the fast modes are integrated forward to the desired point in time using several small time steps $\Delta\tau$ – the slow tendency is fixed. The starting point of the integration $\phi^0_{i,k}$ depends on the chosen variant of the Runge-Kutta scheme – for the first variant it is always equal to $\phi^n_{i,k}$:

1. step:

$$\phi^{0+\Delta\tau}_{i,k} = \phi^0_{i,k} + \Delta\tau\, L^{fast}_{i,k}(\phi^0) + \Delta\tau\, L^{slow}_{i,k}\Big|^\times_0$$

remaining steps:

$$\phi^{\tau+\Delta\tau}_{i,k} = \phi^\tau_{i,k} + \Delta\tau\, L^{fast}_{i,k}(\phi^\tau) + \Delta\tau\, L^{slow}_{i,k}\Big|^\times_0$$

with $\times = *,\ **$ and $n+1$ in the individual Runge-Kutta steps.

Horizontal and Vertical Operators:

$$L^h_i(\phi)^{\,(4\text{th})} = \frac{u_i}{12\Delta x}\Big[\phi_{i-2} - 8\big(\phi_{i-1} - \phi_{i+1}\big) - \phi_{i+2}\Big]$$

$$L^h_i(\phi)^{\,(3\text{rd})} = L^h_i(\phi)^{\,(4\text{th})} + \frac{|u_i|}{12\Delta x}\Big[\phi_{i-2} - 4\big(\phi_{i-1} + \phi_{i+1}\big) + 6\phi_i + \phi_{i+2}\Big]$$

$$L^h_i(\phi)^{\,(6\text{th})} = \frac{u_i}{60\Delta x}\Big[-\phi_{i-3} + 9\big(\phi_{i-2} - \phi_{i+2}\big) - 45\big(\phi_{i-1} - \phi_{i+1}\big) + \phi_{i+3}\Big]$$

$$L^h_i(\phi)^{\,(5\text{th})} = L^h_i(\phi)^{\,(6\text{th})} + \frac{|u_i|}{60\Delta x}\Big[-\phi_{i-3} + 6\big(\phi_{i-2} + \phi_{i+2}\big) - 15\big(\phi_{i-1} + \phi_{i+1}\big) + 20\phi_i - \phi_{i+3}\Big]$$

$$L^v_k(\phi)^{\,(2\text{nd})} = \frac{w_k}{2\Delta z}\big(\phi_{k+1} - \phi_{k-1}\big)$$

2 Idealized Advection Test

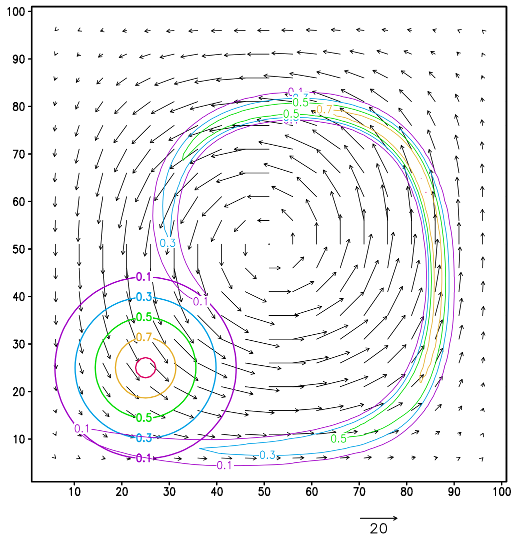

Figure 1: *Advection of a tracer in a non-divergent deformational flow (LeVeque 1996). Thick contours: initial field; thin contours: field after first half of the deformation cycle.*

An test problem of a tracer in a deformational flow field (LeVeque 1996) was used to evaluate the different time integration schemes in combination with varying high-order spatial discretization schemes for advection. The initialized field was a cone with a maximum of 1.0 and a radius of 15 grid spacings. In the first half of the simulation the tracer field is deformed vortex-like (Figure 1). The flow is reversed in the second half of the simulation cycle and the analytical solution at the end would be exactly equal to the initialized field.
The results of the simulations are given in Figure 2. The number of time steps used for the stable integration of one deformation cycle is given in the caption for each scheme. Especially in the combination with centered-differences the TVD-variant shows its benefits. Unfortunately when actually implemented in LM one still has to use a certain amount of numerical smoothing in form of artificial horizontal diffusion to control the small scale oscillations. In this regard the implicit diffusion of the upwind schemes stabilizes the overall integration and even bigger time steps are usable.

3 Test Case: Winter Storm "Lothar"

To test the robustness of the scheme, the winter storm case "Lothar" (26 December 1999) was simulated with the LM. Results are shown in Figure 3. The maximum horizontal velocity during the simulation reaches 108 m/s. For this case the new scheme in the combination TVD-RK-3rd/UP-5th allows a time step of 72 s at a resolution of 7 km compared to a time step of 40 s of the operational Leapfrog/CD-2nd scheme.
This case was also used in simulations to evaluate a new "symmetric" formulation of the thermodynamic equations (described in further detail below). The main change in this formulation lies in the use of a prognostic equation for T^* – the temperature perturbation – instead of the whole temperature T. It was necessary to use a smoother formulation of the relaxation at the lateral boundaries to control numerical problems. In addition the result for a simulation with a higher resolution of 2.8 km is shown.

4 Metric Coefficients and "Symmetric" Thermodynamic Equations

The new the dynamic core uses a different formulation of the metrics. Instead of the former pressure based one a formulation based on the geometrical height is applied:

$$\sqrt{\gamma} \equiv \frac{\partial p_0}{\partial \zeta} \quad \Longrightarrow \quad \sqrt{G} \equiv -\frac{\partial z}{\partial \zeta} = \frac{1}{g \rho_0} \sqrt{\gamma}.$$

In addition, the averaging to the half level positions is now done by a simple arithmetic mean and not a weighted mean any more.

To come to a consistent treatment of the gravity wave modes in the fast waves solver a "symmetric" formulation of the thermodynamic equations was implemented. Therefore we

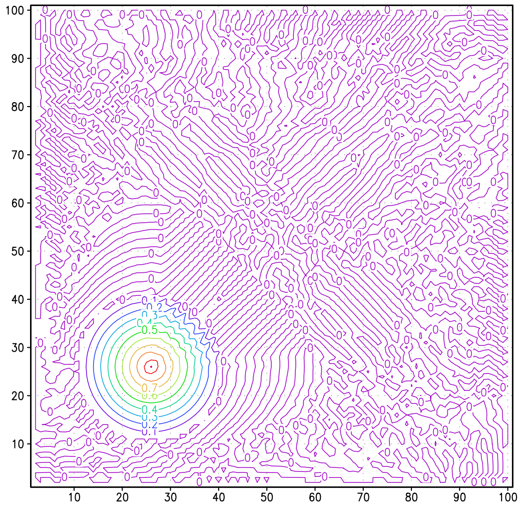

(a) RK-3rd / CD-4th – 670 time steps.

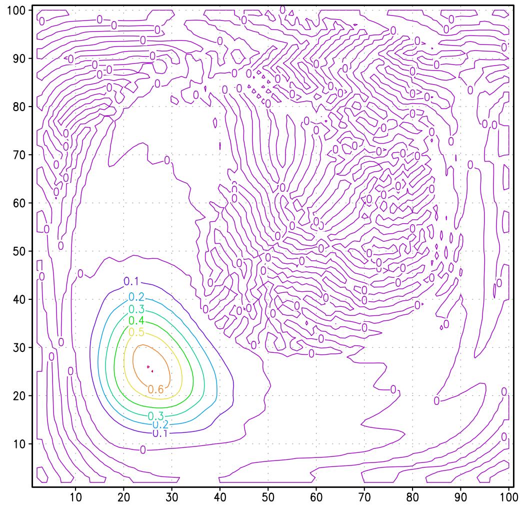

(b) RK-3rd / CD-4th with 4th-order artificial horizontal diffusion – 550 time steps.

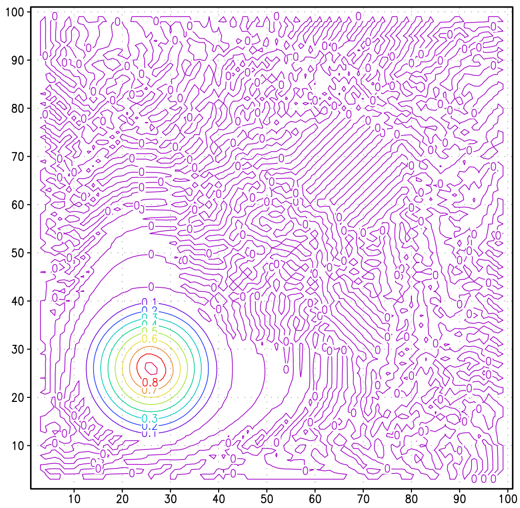

(c) TVD-RK-3rd / CD-4th – 450 time steps.

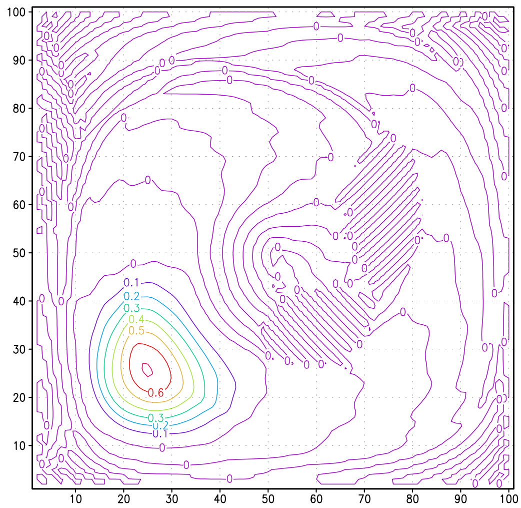

(d) RK-3rd / UP-5th – 380 time steps.

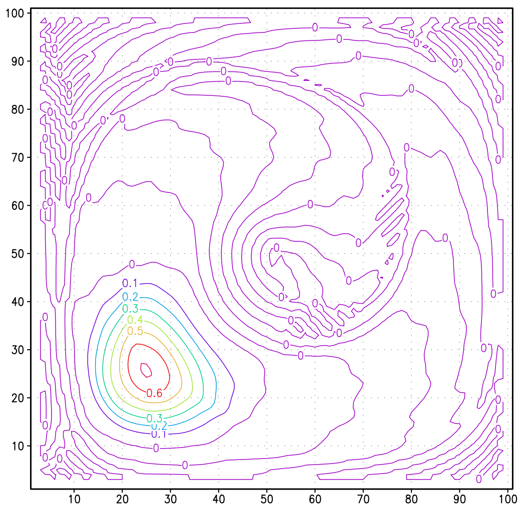

(e) TVD-RK-3rd / UP-5th – 380 time steps.

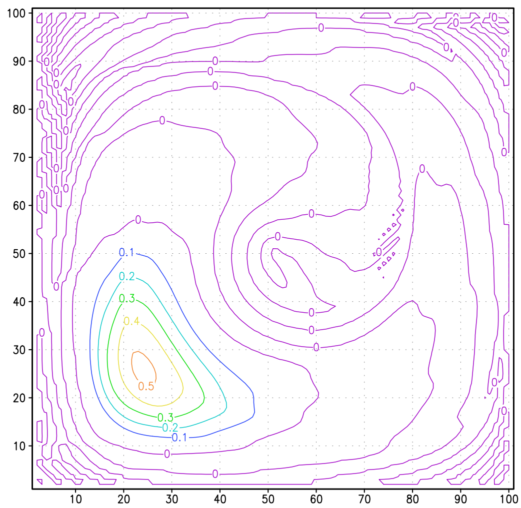

(f) TVD-RK-3rd / UP-3rd – 310 time steps.

Figure 2: *Advection of a tracer in a non-divergent deformational flow (LeVeque 1996). Results after 5 s simulation (one deformation cycle).*

change to a prognostic equation for the temperature perturbation T^*:

$$T \quad \Longrightarrow \quad T^* = T - T_0(z).$$

The resulting term of the advection of the reference temperature T_0

$$\vec{v} \cdot \vec{\nabla} T_0 = -\frac{\mathrm{d}T_0}{\mathrm{d}\ln p_0} \frac{g\rho_0}{p_0} w = \frac{\mathrm{d}T_0}{\mathrm{d}z} w$$

is treated in the fast modes part of the model.

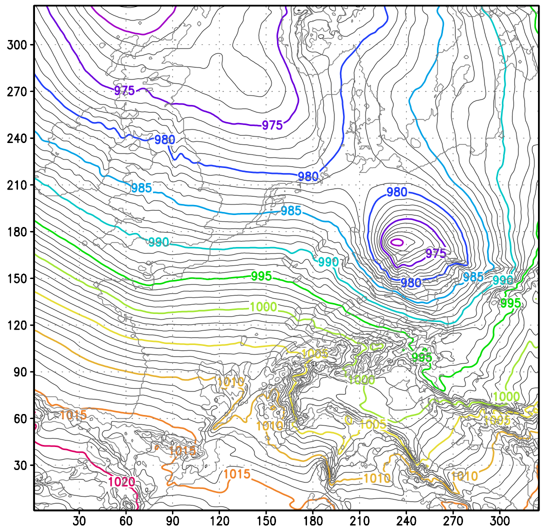

(a) TVD-RK-3rd / UP-5th – $\Delta x, \Delta y$ = 7 km; Δt = 72 s. Prognostic equation for T (standard).

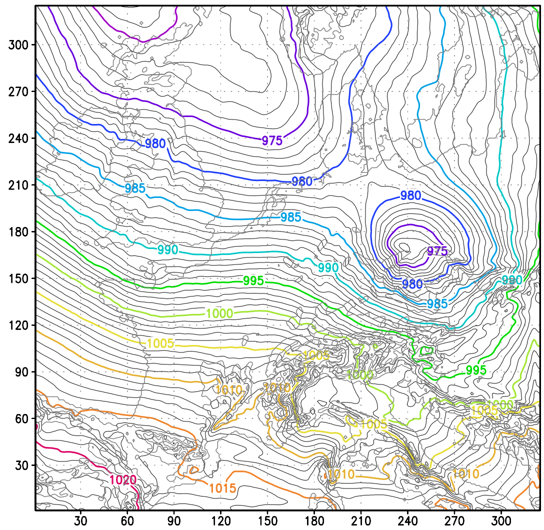

(b) Leapfrog / CD-2nd – $\Delta x, \Delta y$ = 7 km; Δt = 40 s. Prognostic equation for T (standard).

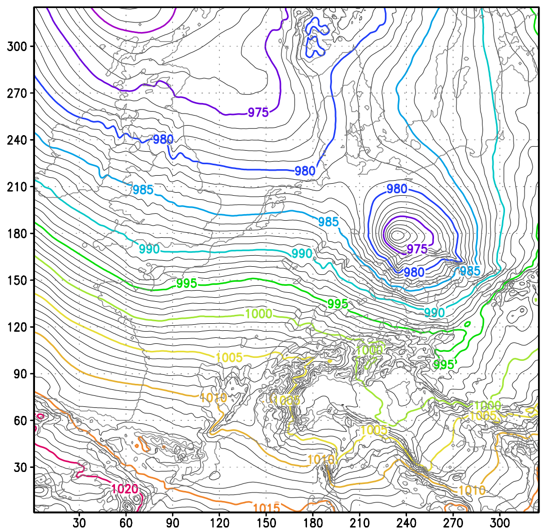

(c) TVD-RK-3rd / UP-5th – $\Delta x, \Delta y$ = 7 km; Δt = 72 s. Prognostic equation for T^*; smoother relaxation LBC.

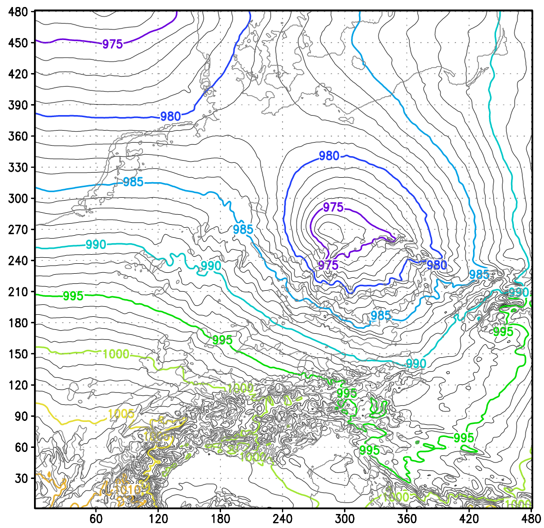

(d) TVD-RK-3rd / UP-5th – $\Delta x, \Delta y$ = 2.8 km; Δt = 30 s. Prognostic equation for T^*; smoother relaxation LBC.

Figure 3: *Winter storm "Lothar": mean sea level pressure in hPa – 26 December 1999, 16 UTC.*

Now the equations for the pressure and temperature perturbation are formulated

$$p^{*(\nu+1)} = \ldots + \Delta\tau g \rho_0 \left(\beta^{+} \overline{w}^{\zeta(\nu+1)} + \beta^{-} \overline{w}^{\zeta(\nu)} \right)$$
$$T^{*(\nu+1)} = \ldots - \Delta\tau \frac{\mathrm{d}T_0}{\mathrm{d}z} \left(\beta^{+} \overline{w}^{\zeta(\nu+1)} + \beta^{-} \overline{w}^{\zeta(\nu)} \right)$$

and semi-implicitly coupled with the prognostic equation of the vertical velocity

$$w^{(\nu+1)} = \ldots - \Delta\tau g \frac{\overline{\rho_0}^{\zeta}}{\overline{\rho^n}^{\zeta}} \left[\overline{\left(\frac{T_0 \beta^{+}}{T^n p_0} \right) p^{*(\nu+1)}}^{\zeta} \overline{\left(\frac{T_0 \beta^{-}}{T^n p_0} \right) p^{*(\nu)}}^{\zeta} \right]$$
$$+ \Delta\tau g \frac{\overline{\rho_0}^{\zeta}}{\overline{\rho^n}^{\zeta}} \left[\overline{\left(\frac{\beta^{+}}{T^n} \right) T^{*(\nu+1)}}^{\zeta} + \overline{\left(\frac{\beta^{-}}{T^n} \right) T^{*(\nu)}}^{\zeta} \right]$$

in a "symmetric" way.

The "symmetric" treatment of the temperature equation is still under development. While several tests look quite promising, others reveal big differences between this and the former treatment. For example tests cases of convective storm development (Weisman and Klemp 1982) – which are not shown here – clearly show the great sensitivity of the model results with respect to the treatment of the buoyancy term. And we do not know yet, which is the correct one – at least in a numerical sense.

5 Mountain Flow: Analytic and Numeric Solutions

As a further test of the different 2-timelevel Runge-Kutta cores 2D-simulations of the flow over a bell shaped mountain were performed and compared to an analytic solution (as well as the old 3-timelevel Leapfrog core). The results are given in Figure 4. For this case the best match with the analytic solution is accomplished with the Runge-Kutta scheme using T^* as prognostic variable. This looks promising for the new "symmetric" treatment, but one has to keep in mind, that the vertical advection of T_0 is equal to zero in this case of an isotherm atmosphere. Therefore the buoyancy-related sensitivity of the model mentioned before has minor influence here.

6 Numerical Experiment: "Testsuite 2"

In addition to the first test suite (see paper by Doms and Förstner, this volume) in another numerical experiment the model with the new dynamical core was run in an operational forecast setup for the period 1 December to 31 December 2003. The Experiment was called "Testsuite 2". Besides the dynamical core the only other change we had to make was to use the old turbulent diffusion and transfer schemes. This was due to numeric instabilities in the new turbulence scheme, which uses a prognostic equation for the TKE to compute the diffusion coefficients.

As an example Figure 5 shows a comparison of the Runge-Kutta and the operational version of the 00 UTC run for 20 December 18 UTC. We see, that the pressure field looks good and corresponds well to the operational version. For precipitation the new core generates systematically smaller amounts in the mean. In this context it is noticeably, when we look at the integrated cloud condensate, that we have less clouds particularly over the sea. Further verification and comparison with precipitation measurements (of high quality) have to show, if that is desirable. The only bigger problem so far – revealed by a quick verification of the first eight days – is a bad forecast of the 2m-temperature. But that is rather an effect of the old turbulence scheme than the new dynamical core.

7 Outlook

In the meantime Matthias Raschendorfer has solved the problems leading to the numeric instabilities and the changes will probably be integrated in the operational source code of LM commencing with version 3.9. The next step is "Testsuite 3" – using the 2.8 km LMK setup, a time step of 30 s, prognostic precipitation, prognostic TKE and certainly the new TVD-Runge-Kutta core combined with 5th-order upwind for horizontal advection.

The ongoing development of LMK aims at the implementation of a 3D-turbulence scheme (Herzog et al. 2003) and further investigation of the "symmetric" formulation of the thermodynamic equations with a set of idealized test cases proposed at the last SRNWP-workshop (Bad Orb, 2003).

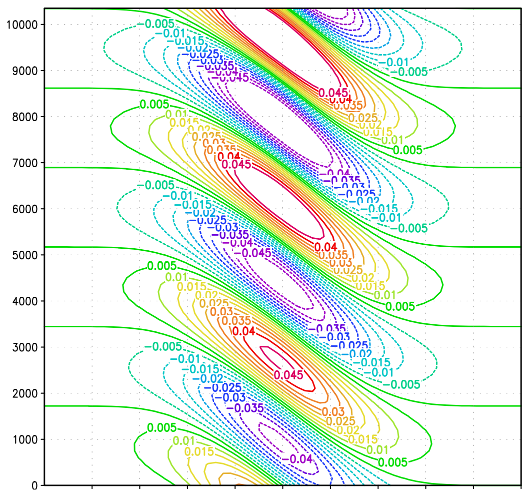

(a) Analytic solution.

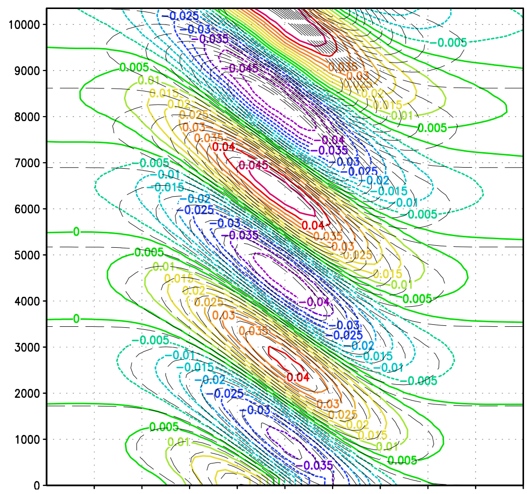

(b) Leapfrog / CD-2nd – Δt = 40 s. Prognostic equation for T (standard).

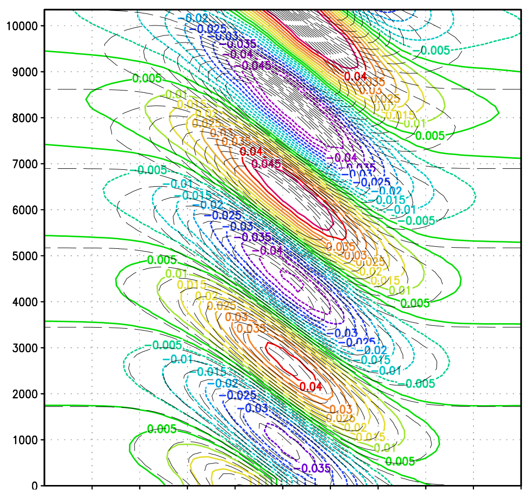

(c) TVD-RK-3rd / UP-5th – Δt = 72 s. Prognostic equation for T (standard).

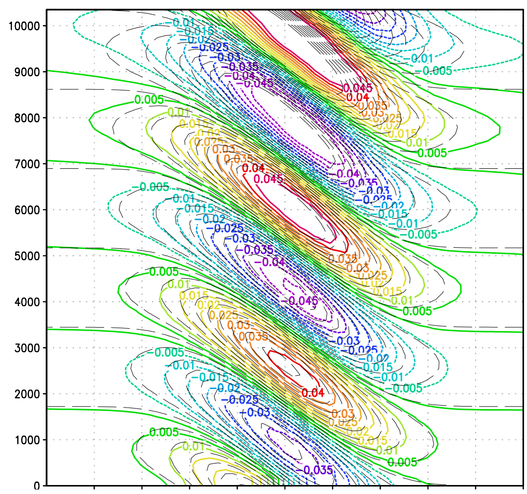

(d) TVD-RK-3rd / UP-5th – Δt = 72 s. Prognostic equation for T^*; smoother relaxation LBC.

Figure 4: *Vertical cross section of 2D flow over a mountain of 100 m height and a half width of 4 grid spacings. Shown is the vertical wind velocity w. Incoming flow:* $U = 10$ *m/s; stratification: isotherm –* $T_0 = 285.15$ *K.*
Fig. (b)-(d): Results of LM simulations after a simulation time of 30 h – $\Delta x, \Delta y = 7$ *km. The analytic solution is given in thin dashed contours.*

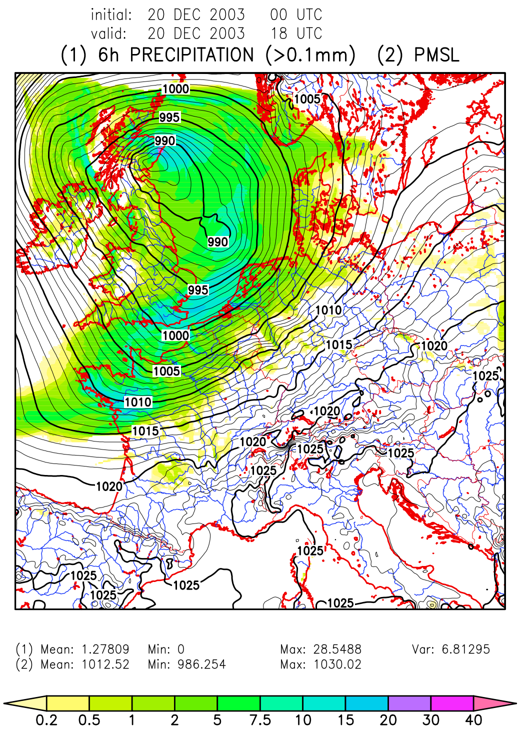

(a) **LM-RK**: Precipitation – 12-18 UTC.

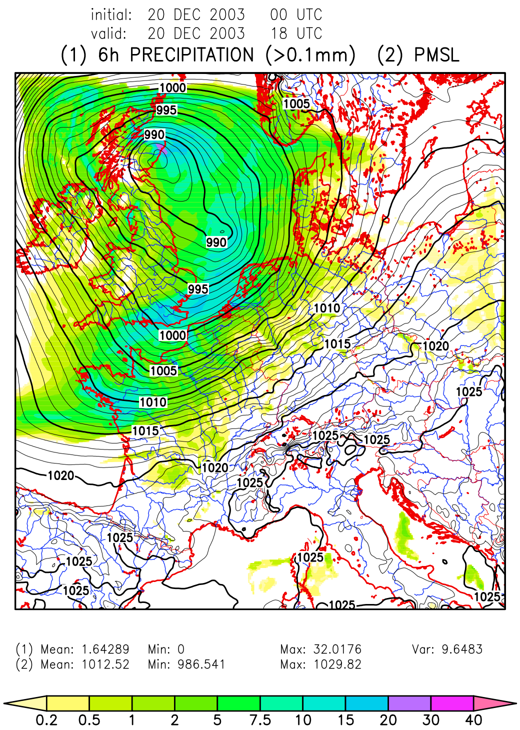

(b) **LM**: Precipitation – 12-18 UTC.

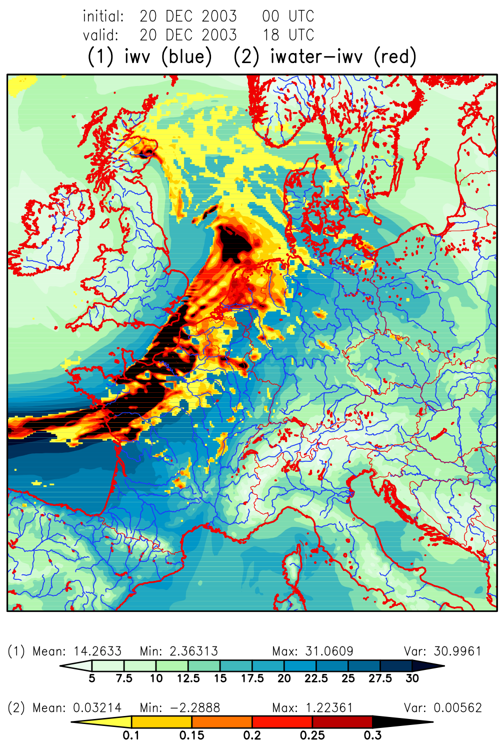

(c) **LM-RK**: Integrated water vapor (green-blue) and cloud water and ice (yellow-red) – 18 UTC.

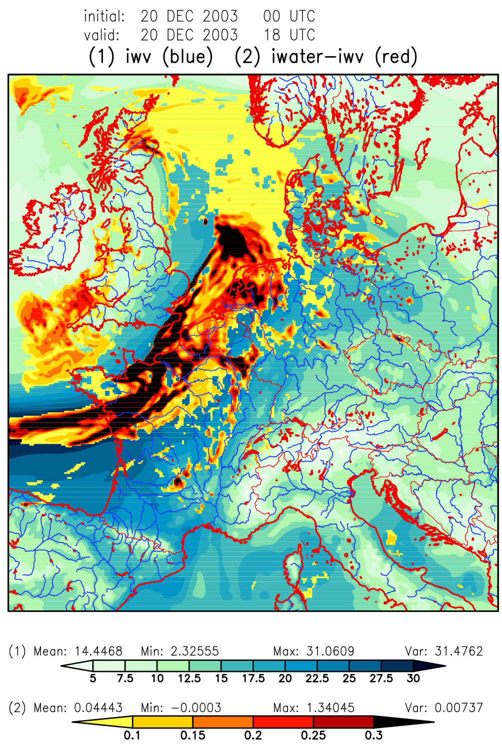

(d) **LM**: Integrated water vapor (green-blue) and cloud water and ice (yellow-red) – 18 UTC.

Figure 5: *Numerical experiment "Testsuite 2" to evaluate the new dynamical core –* $\Delta x, \Delta y =$ *7 km; initial time of the simulation: 20 December 2003 - 00 UTC.*
LM-RK*: New dynamical core – TVD-RK-3rd / UP-5th –* $\Delta t = 72$ *s. Old (diagnostic) TKE scheme (itype_turb=1, itype_tran=1).*
LM*: Routine version – Leapfrog / CD-2nd –* $\Delta t = 40$ *s. Prognostic TKE scheme (itype_turb=3, itype_tran=2).*

8 References

Doms, G. and J. Förstner (2004). Development of a kilometer-scale NWP-system: LMK. In *COSMO Newsletter*, Number 4. Offenbach a. M., Germany: Deutscher Wetterdienst.

Herzog, H.-J., G. Vogel, and U. Schubert (2003). Incorporating a 3D subgrid scale turbulence scheme into the 2.8km-version of the LM. In *COSMO Newsletter*, Number 3, pp. 195–197. Offenbach a. M., Germany: Deutscher Wetterdienst.

LeVeque, R. J. (1996). High-resolution conservative algorithms for advection in incompressible flow. *SIAM J. Numer. Anal. 33*, 627–665.

Liu, X.-D., S. Osher and T. Chan (1994). Weighted essentially non-oscillatory schemes. *J. Comput. Phys. 115*, 200–212.

Weisman, M. L. and J. B. Klemp (1982). The dependence of numerically simulated convective storms on vertical wind shear and buoyancy. *Mon. Wea. Rev. 110*, 504–520.

Wicker, L. J. and W. C. Skamarock (2002). Time-splitting methods for elastic models using forward time schemes. *Mon. Wea. Rev. 130*, 2088–2097.